

# Nuclear-resonance photon scattering study of N<sub>2</sub>O multilayers adsorbed on Grafoil at 12 K

R. Moreh

*Physics Department, Ben-Gurion University of the Negev, Beer-Sheva 84105, Israel  
and Nuclear Research Center-Negev, Beer-Sheva, Israel*

Y. Finkelstein

*Physics Department, Ben-Gurion University of the Negev, Beer-Sheva 84105, Israel  
(Received 20 July 1999; revised manuscript received 4 October 1999)*

The nuclear-resonance photon scattering technique was used for studying the out-of-plane orientation of N<sub>2</sub>O molecules physisorbed on Grafoil at 12 K and coverages  $n=0.77$  to 3.7 monolayers. By monitoring the resonantly scattered intensity ratios from the 6324 keV level in <sup>15</sup>N with the planes of the Grafoil adsorbing surface set parallel and perpendicular to the direction of the incident photon beam, the average out-of-plane tilt of N<sub>2</sub>O relative to the graphite planes was obtained. The behavior of the system reveals a striking similarity to that of the N<sub>2</sub>+Grafoil system. Specifically, the tilt angles of the N<sub>2</sub>O molecules with respect to the graphite surface are practically the same despite its more involved character. It is shown that the occurrence of a pure four-sublattice pinwheel ordering can be ruled out. The possibility of explaining the measured intensity ratios at 12 K, by assuming *partial* dewetting of the N<sub>2</sub>O molecules (where the molecules in the first layer lay flat on the graphite surface while the overlayers consist of highly disordered bulk) is discussed in some detail.

## I. INTRODUCTION

The structural arrangement of molecules, such as N<sub>2</sub>, NO<sub>2</sub>, CO, C<sub>2</sub>H<sub>2</sub>, and C<sub>2</sub>H<sub>4</sub>,<sup>1-5</sup> physisorbed on graphite was extensively studied in relation to two-dimensional physics. In contrast to adsorbed atoms, such nonspherical molecules carry additional degrees of freedom related to their in-plane and out-of-plane orientations relative to the graphite planes. This additional feature gives rise to complex structures<sup>6</sup> like the orientationally ordered 2-in and 2-out herringbone (HB) or pinwheel (PW) configurations and to new types of structural phase transitions. Among all investigated physisorption systems of molecular gases on substrates, N<sub>2</sub>+graphite is considered to be a model system due to its relative simplicity and to the extensive information accumulated from both experimental and theoretical studies. Due to the huge amount of data,<sup>1</sup> there is a broad consensus about the interpretation of the phase diagram obtained for the N<sub>2</sub>+graphite system. The structural richness of the two-dimensional (2D) phase diagrams arises from the subtle balance between the asymmetric adsorbate-substrate potential and the adsorbate-adsorbate quadrupolar interactions. Yet, one interesting feature, incompletely covered by all other techniques is the study of the out-of-plane tilt angle of the molecular symmetry axis relative to the graphite planes. The nuclear-resonance-photon-scattering (NRPS) technique<sup>7</sup> used in the present work is unique in that it provides a very sensitive tool for measuring the out-of-plane tilt angle of adsorbed molecules. It differs from all diffraction methods in providing information not only on that part of the adsorbed gas, which is in a crystalline phase, but on all adsorbed molecules of the gas irrespective of its physical state. Recently, in a measurement<sup>8</sup> of the tilt angle of N<sub>2</sub> monolayers adsorbed on graphite, a detailed out-of-plane tilt behavior was obtained for the N<sub>2</sub>+graphite system, between 0.6–5.0 commensurate monolayers (CML) at 20 K where the multilayer regime was

analyzed relying on *n*-diffraction (ND) results. In this study, the possibility of the occurrence of a PW structure, thought to occur near the fully compressed monolayer coverage, was ruled out.

The principle quantity measured in the present work is the anisotropy ratio  $R$ , of scattered intensities, with the  $\gamma$  beam parallel and perpendicular to the graphite planes of the sample. The NRPS high sensitivity to out-of-plane tilts makes it very easy to distinguish between structures of herringbone, pinwheel, or a combination of both. This point is illustrated by noting that the calculated value of  $R=I_{\parallel}/I_{\perp}$ , at 12 K from <sup>15</sup>N in the form of N<sub>2</sub>O on Grafoil, is  $R\sim 0.97$  for an ideal four-sublattice PW and  $R\sim 1.31$  for a 2-in HB structure.

The linear heteronuclear N<sub>2</sub>O provides yet an additional degree of freedom, i.e., its head-tail ordering. It has a small dipole moment<sup>9</sup> ( $\sim 0.55\times 10^{-30}$  C m) and a large quadrupole moment<sup>9</sup> ( $\sim -1.0\times 10^{-39}$  C m<sup>2</sup>), double that of N<sub>2</sub>. The adsorbed layers are expected to take a structure corresponding to the optimum balance between the holding potential of the graphite substrate, the van der Waals interactions, and the quadrupolar coupling between the molecules. It may be noted that although the NRPS method is highly sensitive to the out-of-plane tilt angle of the adsorbed molecules it is entirely insensitive to the ordering within the plane, or the degree of commensurability on the graphite surface, or to the head-tail ordering. Experimentally, the N<sub>2</sub>O+graphite system was studied by measuring its adsorption isotherms,<sup>10</sup> by calorimetric methods,<sup>11</sup> and by *n* diffraction.<sup>12</sup> However, we found no molecular-dynamics simulations (MDS) studies of the N<sub>2</sub>O+graphite system. Such calculations were extensively used for studying the N<sub>2</sub>+graphite system and many interesting experimental features of this system could be reproduced. Because of the similarity between the N<sub>2</sub>O and N<sub>2</sub> molecules, it would be very interesting to compare the behavior of the N<sub>2</sub>O+graphite system with that of N<sub>2</sub>+graphite

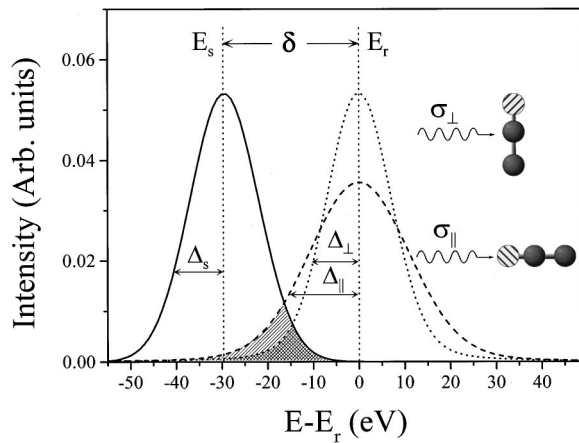


FIG. 1. Calculated shapes of the Doppler-broadened level at 6324 keV in  $^{15}\text{N}$ , of peak energy  $E_r$  and of the Doppler-broadened ( $\Delta_s = 10.6$  eV) incident line of the  $^{53}\text{Cr}(n, \gamma)$  reaction of peak energy  $E_s$  (after recoil correction). The nuclear level shape is depicted for two ideal cases (at  $T = 0$  K), where the  $\text{N}_2\text{O}$  symmetry axis is aligned parallel and perpendicular to the  $\gamma$  beam direction. The corresponding Doppler widths  $\Delta_{\parallel}$  and  $\Delta_{\perp}$  of the two lines are indicated. The overlap integrals between the shapes of the incident line and the nuclear level are shown as shaded areas and correspond to the scattering cross sections  $\sigma_{\parallel}$  and  $\sigma_{\perp}$ .

and to see to what extent their behavior correlate. In the present work we studied the tilt angle of the  $\text{N}_2\text{O}$ -graphite system versus coverage at 12 K, where the thermal motion is practically frozen, and the anisotropy ratios can be viewed as caused mainly by the zero-point kinetic energy of the four internal vibrations of the  $\text{N}_2\text{O}$  molecule.

## II. PRINCIPLE OF THE NRPS TECHNIQUE

Nuclear-resonance photon scattering from N-containing molecules involves a chance overlap between a  $\gamma$  line, generated by the  $^{53}\text{Cr}(n, \gamma)$  reaction, and the 6324 keV nuclear level of  $^{15}\text{N}$ . Both the incident  $\gamma$  line and the nuclear level are Doppler broadened and are separated<sup>7</sup> by  $\delta = 29.5$  eV (Fig. 1). It turns out that the overlap between the two line shapes (Fig. 1) gives rise to a resonance scattering signal whose cross section  $\sigma_r$  is proportional to the Doppler broadening  $\Delta_r$  of the nuclear level, where  $\Delta_r = E(2kT_r/M_r c^2)^{1/2}$  with  $E$  the excitation energy,  $M_r$  the nuclear mass,  $T_r$  the effective temperature of the scattering atom,  $k$  the Boltzmann constant, and  $c$  the velocity of light. A similar definition holds for the Doppler width  $\Delta_s$  of the incident  $\gamma$  line. The effective temperature  $T_r$  gives a measure of the total kinetic energy of the  $^{15}\text{N}$  atom, including that of the zero-point motions.  $\text{N}_2\text{O}$  is a linear molecule with four internal vibrational modes of motion<sup>13</sup> consisting of two stretching modes of the N-N and N-O bonds and antisymmetric bendings of the N-N-O angle. The  $\text{N}_2\text{O}$  used in the present work, was isotopic gas (99%  $^{15}\text{N}$ ) with only one  $^{15}\text{N}$ -labeled atom, namely  $^{15}\text{N}$ - $^{14}\text{N}$ -O (see Fig. 2). The kinetic energy of the  $^{15}\text{N}$  atom contributed by the internal vibrational modes has a maximum along the molecular axis and a minimum along the perpendicular direction (see Fig. 2). This may be understood by noting that the frequencies of the stretching modes (contributing along the  $\text{N}_2\text{O}$  molecular

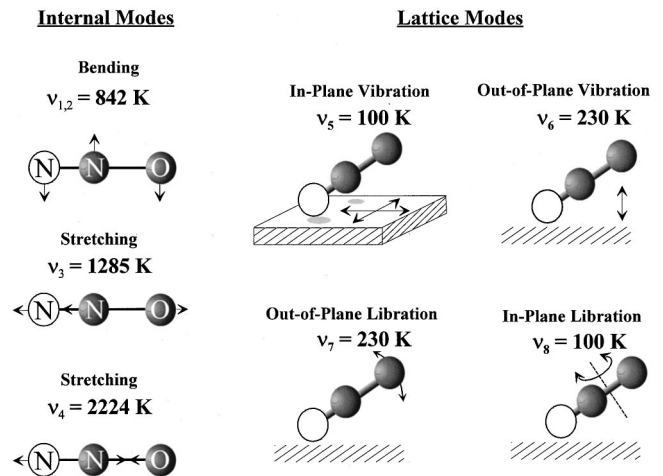


FIG. 2. Schematic representation of the internal and external modes of motion of the  $\text{N}_2\text{O}$ -graphite system. The open circles represent the  $^{15}\text{N}$  resonance scatterer. Note that the  $^{15}\text{N}$ - $^{14}\text{N}$  bond is shorter (Refs. 13 and 25) than the  $^{14}\text{N}$ -O bond by  $\sim 5\%$  only and not as shown. All frequencies are in K units and correspond to the  $^{15}\text{N}$  atom. In the doubly degenerate internal bending mode, the  $^{15}\text{N}$  motion is normal to the  $\text{N}_2\text{O}$  molecular axis, while in the stretching modes (Ref. 14), its motion is along the molecular axis. The external modes ( $j = 5, \dots, 8$ ) are represented by Einstein oscillators [see Eq. (1) of Ref. 8], where arrows indicate the direction of motion of  $\text{N}_2\text{O}$  with respect to the graphite plane. The indicated values of the lattice frequencies ( $j = 5, \dots, 8$ ) were deduced by us empirically, whereas those of the internal motions ( $j = 1, \dots, 4$ ) were taken from Ref. 13.

axis) are a factor of 2–4 higher than those of the bending modes (contributing in the normal direction). Hence the Doppler broadening of the nuclear level has a maximum,  $\Delta_{\parallel}$ , along the  $\text{N}_2\text{O}$  molecular axis and a minimum,  $\Delta_{\perp}$ , perpendicular to it. These correspond to scattering cross sections  $\sigma_{\parallel}$  and  $\sigma_{\perp}$  that are proportional to the overlap integrals (shown as the shaded areas in Fig. 1) and fulfill the relation  $\sigma_{\parallel} \gg \sigma_{\perp}$ . The dependence of the scattering cross section  $\sigma_r$  on the orientation of  $\text{N}_2\text{O}$  with respect to the photon beam is utilized here for measuring the out-of-plane tilt angle of the  $\text{N}_2\text{O}$  molecular axis with respect to the adsorbing graphite planes.

## III. EXPERIMENTAL DETAILS

The  $\text{N}_2\text{O}$ +Grafoil system was studied previously,<sup>14</sup> and the out-of-plane tilt was monitored between 12 and 297 K at two molecular coverages:  $n = 0.77$  and 1.33 monolayers. All the experimental details, including the experimental setup, photon beam properties, details of the  $\gamma$  source, temperature, the Grafoil+ $\text{N}_2\text{O}$  target, and the Ge detectors may be found in Ref. 14. Here we just mention that we used isotopic  $\text{N}_2\text{O}$  of the form  $^{15}\text{N}$ - $^{14}\text{N}$ -O (see Fig. 2). The molecular coverage of  $\text{N}_2\text{O}$  on Grafoil was determined by weighing the amount of adsorbed  $\text{N}_2\text{O}$  gas and comparing its weight with the corresponding amounts of  $\text{N}_2$  in the  $\text{N}_2$ +Grafoil system (determined by vapor pressure measurements<sup>8,15</sup> at 77 K). Thus our calibration point was the weight amount of  $\text{N}_2$  on Grafoil forming one CML; the corresponding amount of  $\text{N}_2\text{O}$  was larger by the mass ratio between  $^{15}\text{N}^{14}\text{NO}$  and  $^{15}\text{N}_2$  being

1.50. It is not clear however whether  $N_2O$  does indeed form a registered  $\sqrt{3}$  triangular lattice on graphite, even though the actual effective area of the  $N_2O$  molecule, found by adsorption measurements<sup>10</sup> was  $\sim 15.1 \text{ \AA}^2$ , which is consistent with that of the registered  $\sqrt{3}$  unit cell ( $15.7 \text{ \AA}^2$ ). In the following we shall thus use the term ‘‘monolayer’’ (ML) to refer to the  $N_2O$  molecular coverages rather than ‘‘commensurate monolayers’’ usually used for the  $N_2$ +Graphite system. The  $N_2O$  was inserted into the adsorption cell in an off-line fashion. This was done by passing calibrated amounts of gas through a valve fitted on the adsorption cell by cooling its lower part to 77 K. The pressure buildup of  $N_2O$  at  $T=300$  K inside the cell was about 100 psi for a loading coverage of 1 ML, and it increased with increasing coverage. The cell was then attached to the cold finger of a variable temperature cryostat (12 K to 300 K). The system was cooled slowly first to 100 K at a rate of  $\sim 0.5$  K/min, then to 12 K at  $\sim 2$  K/min. In some cases, the temperature was raised slowly to 220 K for annealing and then recooled at a rate of  $\sim 0.5$  K/min; the system was left to equilibrate for  $\sim 2$  h prior to starting the measurements. The scattered intensity ratios are averages over several independent measurements.

#### IV. THEORETICAL REMARKS

As mentioned in Sec. II, if the adsorbed molecules are aligned along the  $\gamma$  beam, the scattered intensity is much higher than the case in which the molecular axis is normal to the beam. This fact is being used for deducing the tilt angle of the molecular axis by measuring the scattered intensity ratio  $R=I_{\parallel}/I_{\perp}$  from the 6324 keV level of  $^{15}N$  in the  $N_2O$ +Grafoil system with the  $\gamma$  beam parallel and perpendicular to the Grafoil planes. The measured value of  $R$  is related to the directional Doppler broadenings of the resonance nuclear level, which in turn depend on the effective temperatures of the  $^{15}N$  scatterer in the two perpendicular geometries of the sample. In the following, a brief description of the calculation of the effective temperature of  $^{15}N$  in  $^{15}N^{14}NO$  and of the scattering cross sections are discussed, and the relation to lattice frequencies of the system is given. For a given temperature and coverage, the measured  $R$  also depends on (i) the spatial distribution of molecular tilts and (ii) the mosaic spread of the adsorbing substrate.

The effective temperature  $T_r$  of  $^{15}N$  is related to its total kinetic energy,  $3kT_r/2$ , which include the part contributed by the internal vibrations.  $N_2O$  is a linear molecule having nine kinetic degrees of freedom: three translations ( $3kT_r/2$ ), two rotations ( $kT_R$ ) and the four internal vibrations ( $k\alpha_j/2$ ,  $j=1,\dots,4$ ). The expression for  $T_r$  may thus be written as<sup>14</sup>

$$T_r = S_t T_t + \frac{2}{3} S_R T_R + \frac{1}{3} \sum_{j=1}^4 S_j \alpha_j. \quad (1)$$

$T_t$  and  $T_R$  are the effective temperatures of the translational and librational motions of the entire molecule.  $k\alpha_j/2 = (hv_j/2)[(e^{hv_j/kT} - 1)^{-1} + 1/2]$  is the kinetic energy (assuming an Einstein oscillator) of the  $j$ th internal vibrational mode of motion (with  $v_j$  the corresponding frequency),<sup>13,14</sup> and the factor (1/2) multiplying it arises from the fact that only half the average vibrational energy is kinetic, and only this part contributes to the Doppler broadening of the  $^{15}N$

nuclear level.  $S_t$ ,  $S_R$ , and  $S_j$  are the energy fractions shared by the  $^{15}N$  atom in the translational, rotational, and vibrational motions of  $^{15}N^{14}NO$ . Thus,  $S_t=15/45$  is obtained from the mass ratio,  $M(^{15}N)/M(^{15}N^{14}NO)$ . Similarly,  $S_R=0.4982$  is obtained from the atomic distances in  $N_2O$  as the fraction of the rotational energy of  $^{15}N$  in that of the  $N_2O$  molecule.<sup>14</sup> The fractions  $S_j$  of the internal vibrational modes (Fig. 2) were obtained using computational methods of molecular spectroscopy.<sup>13</sup> For a pure  $N_2O$  gas, namely, for  $T > 182$  K, Eq. (1) may be rewritten as<sup>14</sup>

$$T_r = S_t T + \frac{1}{3} \sum_{j=1}^4 S_j \alpha_j \quad (2)$$

with  $S_t=(S_t+2S_R/3)$ , the kinetic-energy fraction of the  $N$  atom in the external modes of motion of  $N_2O$ , and  $T$  the thermodynamic temperature. This yields

$$T_r \sim 0.665T + 288 \quad (3)$$

implying that the zero-point kinetic energy of vibration of  $^{15}N$  in  $N_2O$  is  $T_r=288$  K, which contributes to the Doppler broadening of the nuclear level. At 297 K,  $T_r=486$  K, of which 59% arise from the zero-point energy.

Equation (1) gives an idea of calculating the effective temperature of  $^{15}N$  for a nonoriented sample, where the system and hence the scattered intensity is isotropic. However, when dealing with adsorbed  $N_2O$  on oriented graphite, we may calculate the scattered intensities by following two steps. In the first, we calculate the scattered intensities by assuming that the  $N_2O$  is adsorbed on a fully oriented graphite sample. Having done that, we go to the second step in which the scattering cross sections and hence the intensity ratios  $R$  are modified by accounting for the actual structure of the Grafoil substrate. The first step is carried out by defining two effective temperatures of  $^{15}N$ :  $T_a$  and  $T_c$  along and normal to the plane of an assumed fully oriented graphite sample. To do that, we consider a single  $^{15}N^{14}NO$  molecule with its axis tilted at an average angle  $\bar{\theta}$  relative to the graphite plane; the same tilt angle is assumed irrespective of the head-tail ordering.  $T_a$  and  $T_c$  are deduced by projecting the motion of the  $^{15}N$  atom along and perpendicular to the graphite plane, yielding<sup>14</sup>

$$T_a = \left( 0.5 \sum_{j=3,4} S_j \alpha_j \right) \cos^2 \bar{\theta} + 0.5(S_1 \alpha_1 + S_2 \alpha_2 \sin^2 \bar{\theta}) + S_t \alpha_5 + (S_R/2)(\alpha_8 + \alpha_7 \sin^2 \bar{\theta}), \quad (4)$$

$$T_c = \left( \sum_{j=3,4} S_j \alpha_j \right) \sin^2 \bar{\theta} + (S_2 \alpha_2 + S_R \alpha_7) \cos^2 \bar{\theta} + S_t \alpha_6, \quad (5)$$

where  $\alpha_1$ ,  $\alpha_2$  and  $\alpha_3$ ,  $\alpha_4$  are related to the internal bending and stretching modes of  $N_2O$ , respectively. The remaining energy terms are the lattice modes of the  $N_2O$ +graphite system represented by five Einstein oscillators (see Fig. 2): (i) two in-plane degenerate vibrations  $v_5$  (ii) an out-of-plane vibration  $v_6$ , (iii) an out-of-plane libration  $v_7$ , and (iv) one in-plane libration  $v_8$ . The kinetic energies ( $k\alpha_j/2$ ,  $j=5,\dots,8$ ) are defined in a similar manner to those of the internal modes. In deducing  $T_a$  and  $T_c$ , we assumed a de-



coupling between the in-plane and out-of-plane degrees of freedom of motion of  $N_2O$  relative to the graphite surface.

Equations (4) and (5) may also be used for deducing  $T_r$  for the case of a nonoriented ( $N_2O$ +graphite) sample as

$$T_r = (2T_a + T_c)/3. \quad (6)$$

Equation (6) is useful because Grafoil is known to consist of a nonoriented fraction,  $f=0.44$ , of crystallites, whereas the remaining fraction  $(1-f)$  is characterized by a half width at half maximum (HWHM) mosaic spread angle  $\phi_0=15^\circ$ . The value,  $f=0.44$ , for our Grafoil sample was deduced by noting that the  $N_2$  molecular axes lay flat on the graphite surface at  $n < 1$  and low  $T$ , and by requiring that the calculated  $R = I_{\parallel}/I_{\perp}$  of the  $N_2$ +Grafoil system must be equal to the measured  $R$  (see Ref. 15). Next, the scattering cross sections from  $^{15}N$  along and perpendicular to the fully oriented graphite plane is obtained from a knowledge of  $T_a$  and  $T_c$  and the parameters of the nuclear level as explained in detail elsewhere.<sup>7,14</sup>

We now turn to the second step of calculating the scattering cross sections from  $^{15}N^{14}NO$  adsorbed on Grafoil with the photon beam parallel and perpendicular to graphite planes. The Grafoil structure may be accounted for by defining another two effective temperatures  $T_a(\Omega)$  and  $T_c(\Omega)$  of  $^{15}N$  in the form of  $^{15}N^{14}NO$  related to the two perpendicular geometries of the Grafoil planes relative to the beam direction. The spatial angle  $\Omega$  between the  $N_2O$  molecular axis and the beam direction may be expressed in terms of (1) the  $N_2O$  tilt angle  $\bar{\theta}$  with respect to a certain graphite crystallite plane, (2) the orientation  $\phi$  of the crystallite with respect to the Grafoil  $c$  axis, and (3) the azimuthal angle  $\zeta$  of a given molecule relative to the  $\gamma$  direction. Finally, the scattering cross sections  $\bar{\sigma}_{\parallel}(\bar{\theta})$  and  $\bar{\sigma}_{\perp}(\bar{\theta})$  with the  $\gamma$  beam parallel and perpendicular to the Grafoil planes are obtained by integration over  $\zeta$  and  $\phi$  to account for the Grafoil structure. In this manner, the anisotropy ratio  $R = I_{\parallel}/I_{\perp} = \bar{\sigma}_{\parallel}(\bar{\theta})/\bar{\sigma}_{\perp}(\bar{\theta})$  was obtained as discussed in detail in Ref. 8. With this procedure we obtained for the  $N_2O$ +Grafoil system:  $R=0.97$  for a pure PW structure and 1.31 for a 2-in HB structure.

Finally, it should be emphasized that the present method<sup>8</sup> of calculating  $R$  is more accurate than that of Ref. 14. In this latter work the scattering cross section from the 6324 keV level in  $^{15}N$  was assumed to be linearly proportional to the effective temperature of  $^{15}N$  for the entire temperature range. This assumption is not correct at low effective temperatures where a flattening of the scattering cross section occurs. When this assumption was abandoned in Ref. 8, the fitting of the calculated values of  $R$  to the measured data yielded reliable frequencies of the  $N_2$ +graphite lattice modes. Thus the average in-plane and out-of-plane lattice modes (of librations and vibrations),  $v_1 \sim 70$  K and  $v_2 \sim 80$  K (in the solid phase), were found to be in excellent agreement with those calculated<sup>16</sup> theoretically using lattice-dynamic simulations. Those values are much lower than those deduced empirically in the original NRPS work<sup>15</sup> on the  $N_2$ +graphite system.

This same method of calculation was applied to the  $N_2O$ +grafoil system, and the characteristic in-plane and out-of-plane lattice modes (of vibrations and librations) of the adsorbed  $N_2O$  molecules in the solid phase were deduced to be  $v_5 = v_8 = 100$  and  $v_6 = v_7 = 230$  K, respectively (Fig. 2),

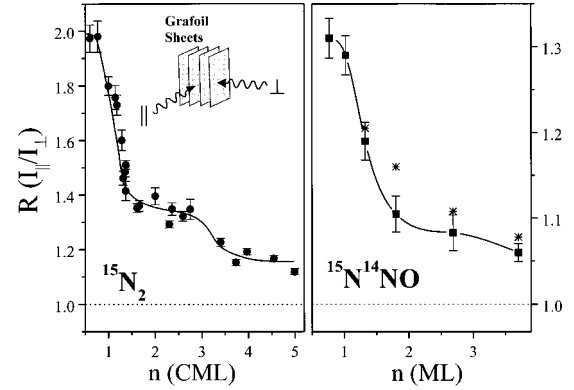


FIG. 3. Measured anisotropy ratios  $R = I_{\parallel}/I_{\perp}$  of the scattered intensities from the  $N_2O$ + Grafoil system (squares) versus the molecular coverage  $n$ , taken at 12 K. The solid line was passed through the data points to lead the eye. Similar data for the  $N_2$ +Papyex system (circles), at 20 K, were taken from Ref. 8. Note the stepwise behavior and the huge difference in the values of  $R$  in the two systems. The stars denote the calculated values of  $R$  for a case where partial dewetting of the  $N_2O$  overlayers is assumed while retaining the original tilt of the first ML. The dashed line at  $R=1$  represents the ratio for nonoriented samples. The inset in the  $^{15}N_2$  case illustrates schematically the two perpendicular geometries of the samples relative to the  $\gamma$  beam direction.

almost a factor of 2 lower than those deduced in the previous work.<sup>14</sup> The fact that the present  $N_2O$ +graphite lattice values are larger than those of  $N_2$ +graphite is due to the much stronger intramolecular interactions as reflected in the much higher melting point,  $T_{2c} \sim 110$  K of  $N_2O$  on graphite.<sup>10</sup>

It is important to note that in spite of the different procedure, the main conclusions obtained in Ref. 14, for the average out-of-plane tilt angles at  $n=1$  ML assuming a 2-in HB structure, remain intact, and only small differences as to the deduced tilt angle occurred. This is due to the dominant contribution of the internal vibrational frequencies in  $N_2O$ , which determine the out-of-plane tilt, and are about one order of magnitude higher than those of the external lattice modes (see Fig. 2).

## VI. RESULTS AND DISCUSSION

Figure 3 shows the measured ratios  $R$  of the scattered intensities versus  $n$ , the molecular coverage (at 12 K) from the two perpendicular geometries of the  $N_2O$ +Grafoil sample with respect to the beam direction (squares). These  $R$  values were used to deduce the average out-of-plane tilt angle  $\bar{\theta}$  of the  $N_2O$  molecular axis versus  $n$  at 12 K (see Fig. 4). The behavior of the ratios  $R$  may be interpreted as follows. At low  $T$  and submonolayer coverages ( $n = 0.77$  ML),  $R$  has a maximum ( $R \sim 1.31$ ) that corresponds to a tilt of  $\bar{\theta} \sim 3.0^\circ \mp 2.0^\circ$ , representing  $N_2O$  molecules lying flat on the graphite surface. When  $n$  increases,  $R$  decreases slightly to  $R \sim 1.29$  around 1 ML completion. A relatively steep drop to  $R \sim 1.19$  at  $n \sim 1.31$  ML occurs where a sharp out-of-plane ‘‘jump’’ of the  $N_2O$  molecular axes to  $\bar{\theta} \sim 16.3^\circ \mp 1.0^\circ$  occurs. On increasing  $n$  to 1.8 ML,  $R$  reached a value of  $\sim 1.10$  corresponding to  $\bar{\theta} = 22.0^\circ \mp 1.0^\circ$  and then

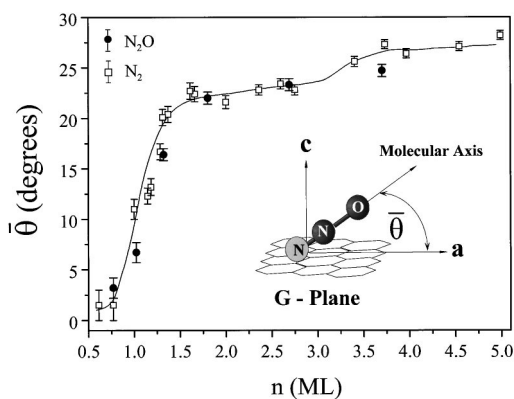


FIG. 4. Deduced average out-of-plane tilt  $\bar{\theta}$  at 12 K of the  $\text{N}_2\text{O}$  molecular axes with respect to the graphite plane (solid circles) versus the molecular coverage  $n$ . The tilt  $\bar{\theta}$  is schematically defined in the inset, with the resonance scattering  $^{15}\text{N}$  atom drawn differently. The solid line was passed through the data points to lead the eye. The data points of the  $\text{N}_2$ +Papyex system (Ref. 8) (open squares) are also shown. Note the remarkable similarity between the two systems.

decreased further to 1.06 at  $n \sim 3.7$  ML where the tilt is  $\bar{\theta} = 24.7^\circ \pm 1.0^\circ$ . The dotted line in Fig. 3 at  $R = 1.0$ , represents the anisotropy ratio for the case where the  $\text{N}_2\text{O}$  molecules are randomly oriented ( $I_{\parallel} = I_{\perp}$ ). The fact that all our  $R$  values are considerably higher than unity, implies that up to the highest measured coverage, the  $\text{N}_2\text{O}$  molecules have, on the average, a definite forward tilt relative to the graphite surface. The fact that around 44% of the crystallites in Grafoil are randomly oriented and the remaining 56% have a mosaic spread of  $15^\circ$  at HWHM reduced markedly the anisotropy ratios.

It is important to emphasize that the deduced values of  $\bar{\theta}$  are useful only for  $n \approx 1$  ML where all the surface molecules are assumed to have the same out-of-plane tilt. At multilayer coverages, the various layers usually have different average tilts as shown in the neutron-diffraction study of the  $\text{N}_2$ +Grafoil system<sup>17</sup> where the first layer was found to have a definite forward tilt, while the molecules in the second layer and higher layers were mostly disordered.

It is interesting to compare the tilt  $\bar{\theta}$  versus  $n$  of the present system, taken at 12 K, with that of the  $\text{N}_2$ +Graphite system<sup>8</sup> taken at 20 K. Figure 4 reveals a striking quantitative similarity whereby the values of  $\bar{\theta}$  are found to follow practically the same  $n$  dependence at low  $T$  and lay on the same smooth curve, passed through the data to lead the eye. This similarity occurs in spite of the nonzero dipole moment and much larger quadrupole moment of  $\text{N}_2\text{O}$ . A much better agreement could have been obtained by artificially rescaling the  $\text{N}_2\text{O}$  coverages, by reducing all coverages corresponding to  $n \geq 1$  ML, by 5%. Such a displacement could be justified if one keeps in mind that the overall uncertainty<sup>1</sup> in the reported coverages (depending on the definition and the method of measurement) is  $\sim 5\%$  at  $n \leq 1$  ML, and  $\sim 25\%$  above 1 ML. The behavior of the two systems should be contrasted to those of the  $\text{NO}$ +Grafoil (Ref. 18) or  $\text{NO}_2$ +Grafoil,<sup>2</sup> where  $R < 1$  was measured for most of the coverages. The remarkable closeness of the tilt angles  $\bar{\theta}$  in the two systems suggests a similar interpretation of the data.<sup>8</sup>

Thus, the strong increase of  $\bar{\theta}$ , occurring between 0.8 and 1.3 ML seem to indicate a phase transition in which monolayer compression seems to take place. Another structure that could be tested is the pure pinwheel, theoretically predicted for linear nonpolar molecules,<sup>6</sup> where each pin ( $\bar{\theta} = 90^\circ$ ) molecule in the unit cell is surrounded by three molecules lying flat on the surface ( $\bar{\theta} = 0^\circ$ ). Our calculated  $R$  for such a pure PW structure of  $\text{N}_2\text{O}$  on Grafoil, at 12 K [Eq. (12) of Ref. 8] is  $R \sim 0.97$ . This is far lower than any of the measured  $R$  values up to a coverage of  $n \sim 3.7$  ML. Obviously, as predicted theoretically<sup>19</sup> and shown experimentally,<sup>8,17</sup> for  $\text{N}_2$  on graphite, the wheel molecules in such an assumed PW structure could have a finite out-of-plane tilt which further reduces  $R$  below 0.97. Alternatively, a combined structure consisting of PW underlayers coexisting with highly disordered overlayer<sup>17,20</sup> would increase the value of  $R$  to  $\sim 1.0$  at the most.<sup>8</sup> Thus, our results indicate that a pure PW ordering cannot occur in the  $\text{N}_2\text{O}$ +graphite system at 12 K and between 0.77 to 3.7 ML.

These facts may motivate new calculations based on MD simulations in a similar fashion to the  $\text{N}_2$ +graphite system.<sup>16,19-23</sup> Although the polarity may not play an important role in the molecular orientational ordering, the comparison between the two system may yield a deeper insight and understanding of the role of the quadrupole moments in determining orientational ordering of adsorbed linear molecules on surfaces.

Another alternative explanation for the above behavior of  $R$ , at  $n > 1$  ML, is the possible occurrence of partial dewetting of molecules forming bulk  $\text{N}_2\text{O}$ . In such a process, which could occur below the 2D melting transition<sup>10</sup> (at  $\sim 110$  K), it is assumed that all excess molecules above 1 ML transforms into a highly disordered bulk while the first ML retains its original tilt. The predicted values of  $R$  for this scenario, in the coverage regime  $n = 1.3-3.7$  ML (indicated as stars in Fig. 3) reveal, apart from the data point at  $n = 1.8$  ML, a reasonable agreement with experiment. It may be noted, however, that the possibility of complete dewetting of the surface, as observed in the  $\text{CO}_2$ +Grafoil system<sup>24</sup> may be ruled out. This is because bulk adsorption is likely to be nonoriented as it is expected to be in a highly amorphous state. Such a situation occurs in the  $\text{N}_2$ -Grafoil system<sup>17</sup> and obviously leads to  $R = 1$ , in contrast to the present results. It should be admitted that this interpretation suffers from some difficulties because only a small change in  $R$  was observed above the 2D melting transition, when the temperature was increased between 12 K to  $\sim 150$  K as reported in Ref. 14.

Another feature worth discussing concerns the question whether the  $\text{N}_2\text{O}$  monolayer on graphite forms a registered  $\sqrt{3}$  structure with the molecular axis parallel to the graphite plane. This point is interesting because of the striking similarity between the present results and those of  $\text{N}_2$  on graphite<sup>8</sup> where a CML is known to form. Another point is that the effective area of  $\text{N}_2\text{O}$  is  $\sim 15.9 \text{ \AA}^2$  as may be seen by noting that the long diameter of the  $\text{N}_2\text{O}$  molecule is  $\sim 5.3 \text{ \AA}$ , consisting of the bond lengths:<sup>25</sup>  $d_{\text{N-N}} = 1.125 \text{ \AA}$ ,  $d_{\text{N-O}} = 1.190 \text{ \AA}$ , and the Van der Waals (VDW) diameter<sup>26,27</sup> of N and O being  $\sim 3.0 \text{ \AA}$ . This means that  $\text{N}_2\text{O}$  could form a  $\sqrt{3}$  registered structure with a 2-in HB ordering at low  $T$  and 1 ML coverage. In fact, Terlain and Larher<sup>10</sup> speculated the

possible occurrence of the  $\sqrt{3}$  structure for the  $N_2O$ +graphite system based on adsorption isotherm measurements. Further evidence may also be found in the ND study<sup>12</sup> of the  $N_2O$ +Grafoil system at 90 K where a triangular  $\sqrt{3}$  structure was reported and an upper limit for the out-of-plane tilt was set at  $\bar{\theta} \sim 10^\circ$ . However, Inaba, Shirakami, and Chihara,<sup>11</sup> relying on calorimetric data at submonolayer coverage between 4 to 130 K, have questioned the existence of the commensurate  $\sqrt{3}$  structure, from arguments on the phonon density of states. Thus, this point remains an open question waiting further experiments.

## VII. CONCLUSIONS

Using the NRPS technique, the average out-of-plane tilt angle  $\bar{\theta}$  of  $N_2O$  adsorbed on graphite at 12 K was determined versus molecular coverage. The tilt was found to increase on increasing molecular coverage and to behave essentially the same, qualitatively and quantitatively, as that measured for the  $N_2$ +Grafoil system at 20 K. The ‘‘jump’’ in the out-of-plane tilt, observed between 0.77 to 1.3 ML, could indicate a phase transition in which the monolayer is compressed beyond its 1 ML density in the same manner as that of the

$N_2$ +Grafoil system. Moreover, the occurrence of a pure four sublattice PW structure in this system was ruled out. It is of interest to note that in spite of the fact that the  $N_2O$  molecule is longer and has a higher quadrupole moment than the  $N_2$  molecule, the low- $T$  behavior of the tilt angle of the two systems is practically the same. It is worth noting that the present  $N_2O$  results may also be understood by assuming a partial dewetting behavior whereby the first ML is orientationally ordered and is coexisting with an overlayer structure consisting of bulk  $N_2O$  below the 2D melting transition. More experimental and theoretical studies of the  $N_2O$ +graphite system could help to resolve the low- $T$  layering structure of  $N_2O$  on graphite. It may also lead to a deeper understanding of the dewetting process, multilayer growth, and the role of the quadrupole moment in determining the structural arrangement of molecules in those systems.

## ACKNOWLEDGMENTS

We would like to thank Y. Feuerlicht and D. Kalir for their technical assistance during the course of this work. This research was supported by the German-Israeli Foundation for Scientific Research and Development (GIF).

- 
- <sup>1</sup>D. Marx and H. Wiechert, *Adv. Chem. Phys.* **XC**, 213 (1996).  
<sup>2</sup>R. Moreh, Y. Finkelstein, and H. Shechter, *Phys. Rev. B* **53**, 16 006 (1996).  
<sup>3</sup>A. Inaba, T. Shirakami, and H. Chihara, *J. Chem. Thermodyn.* **23**, 461 (1991).  
<sup>4</sup>J. Menaucourt, A. Thomy, and X. Duval, *J. Chim. Phys. Phys.-Chim. Biol.* **77**, 959 (1980).  
<sup>5</sup>V. L. Eden and S. C. Fain, Jr., *Phys. Rev. B* **43**, 10 697 (1991).  
<sup>6</sup>A. J. Berlinsky and A. B. Harris, *Phys. Rev. Lett.* **40**, 1579 (1978).  
<sup>7</sup>R. Moreh, O. Shahal, and V. Volterra, *Nucl. Phys. A* **262**, 221 (1976).  
<sup>8</sup>Y. Finkelstein, R. Moreh, and O. Shahal, *Surf. Sci.* **437**, 265 (1999).  
<sup>9</sup>D. E. Stogryn and A. P. Stogryn, *Mol. Phys.* **11**, 371 (1966).  
<sup>10</sup>A. Terlain and Y. Larher, *Surf. Sci.* **125**, 304 (1983).  
<sup>11</sup>A. Inaba, T. Shirakami, and H. Chihara, *Surf. Sci.* **242**, 202 (1991).  
<sup>12</sup>F. Angerand, Commissariat A L'energie Atomique, Report No., IF CEA-R-541 1988 (unpublished), p. 192.  
<sup>13</sup>G. Herzberg, in *Infrared and Raman Spectra* (Van Nostrand Reinhold, New York, 1968).  
<sup>14</sup>R. Moreh and O. Shahal, *Phys. Rev. B* **40**, 1926 (1989).  
<sup>15</sup>R. Moreh and O. Shahal, *Surf. Sci.* **177**, L963 (1986).  
<sup>16</sup>T. H. M. van der Berg and A. Van der Avoird, *Phys. Rev. B* **43**, 13 926 (1991).  
<sup>17</sup>R. Wang, S. K. Wang, H. Taub, J. C. Newton, and H. Shechter, *Phys. Rev. B* **39**, 10 331 (1989).  
<sup>18</sup>R. Moreh and D. Levant, *Mol. Phys.* **69**, 735 (1990).  
<sup>19</sup>C. Peters and M. Klein, *Mol. Phys.* **54**, 895 (1985).  
<sup>20</sup>J. Talbot, D. J. Tildesely, and W. A. Steele, *Faraday Discuss. Chem. Soc.* **80**, 91 (1985).  
<sup>21</sup>A. V. Vernov and W. A. Steele, *Surf. Sci.* **171**, 83 (1986).  
<sup>22</sup>B. Kuchta and R. D. Ethers, *Phys. Rev. B* **36**, 3400 (1987).  
<sup>23</sup>V. R. Bhethanabotla and W. A. Steele, *J. Chem. Phys.* **91**, 4346 (1989).  
<sup>24</sup>K. Morishige, *Mol. Phys.* **78**, 1203 (1993).  
<sup>25</sup>A. S. Parkes and R. E. Hughes, *Acta Crystallogr.* **16**, 734 (1963).  
<sup>26</sup>A. Bondi, *J. Phys. Chem.* **68**, 441 (1964).  
<sup>27</sup>R. E. W. Bader, W. H. Henneker, and P. E. Cade, *J. Chem. Phys.* **46**, 3341 (1967).